The 2014 World Congress on
Advances in Civil, Environmental, and Materials Research (ACEM14)
Busan, Korea, August 24-28, 2014

Material Topology Optimization Design with Regularization of Node Density Design Variables

*Dong-Kyu Lee[1] and Soo-Mi Shin[2]

[1] *Department of Architectural Engineering, Sejong University, Seoul, 143-747, Korea*
[2] *Research Institute of Industrial Technology, Pusan National University, Busan, 609-735, Korea*
[1]* *dongkyulee@sejong.ac.kr*

ABSTRACT

This study shows a combined approach of material topology optimization and a special kind of shape optimization with nodal density values as design parameters. The results of optimal shape and topology presented in the paper are based on density functions interpolated by element shape functions and nodal densities. The material interfaces between void and solid regions are represented by continuous and smooth iso-lines of the density functions in fixed grids. This approach allows us to perform a nodal-based topology and shape optimization, which can be easily implemented in existing gradient-based optimization codes. Numerical examples demonstrate the efficiency of the present method.

1. INTRODUCTION

Using finite element method for structural analysis in material-based topology optimization, material properties are usually assumed to be uniform within one finite element. In this case, the optimization design variables are the densities of finite elements and the final design is described by “0-1” raster patterns. On the one hand this results in very rough layouts depending on the discretization of the design domain. An increase of the number of finite elements will improve the resolution of topology optimization, but is not very efficient. On the other hand the jagged boundaries as shown in Figure 1 cause artificial stress singularities which have an influence on the structural analyses and the optimization process.

To overcome these difficulties different methods were investigated in order to obtain smooth shapes. The adaptive topology optimization method (ATO) (Maute et al. 1988) starts with conventional material based topology optimization. After some optimization

[1] Professor, Ph.D
[2] Post-doctoral researcher, Ph.D

steps a smooth boundary is determined. Additional topology optimization steps with a new discretization are performed within this domain or the result is improved by a shape optimization adjusting the smooth boundary. Although this method works very well for two-dimensional problems (Maute et al. 1988; Kemmler et al. 2005; Schwarz et al. 2001) it is difficult to extend the procedure to the general three-dimensional case for lack of reliable mesh generators.

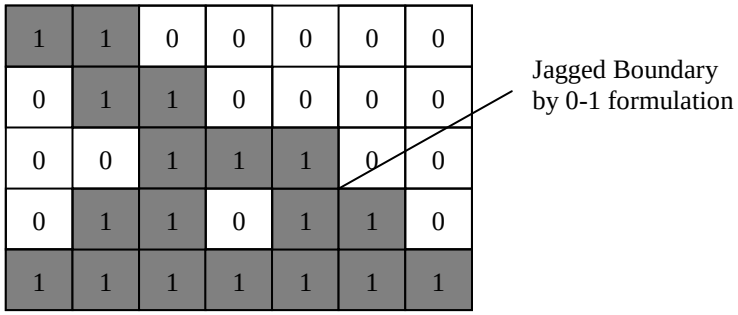

Fig 1. Jagged boundary by 0-1 formulation

Apart from that level set methods have recently been introduced in the field of topology and shape optimization (Allaire et al. 2004; Sethian and Wiegmann 2000). The advantage of smooth boundaries is combined with high numerical efficiency due to working on fixed regular meshes. These methods are designed to describe the propagation of interfaces which separates two phases from each other. In case of topology optimization these interfaces separate the void from the solid phase. However it is difficult for new holes to be introduced in solid regions and no material can be arranged in void regions. For numerical stability the length of time steps has to be limited so that the level sets do not move more than one grid length by which the convergence may slow down.

In this study a method will be presented to overcome these problems. Most often a constant density within a finite element is used. In contrast to this procedure, here the density values are interpolated by element shape functions and are used as design parameters in material topology optimization. This increase of design parameters results in a layout which is much more detailed than using constant element densities as design parameters. It also avoids checkerboard patterns in case of low order finite elements. Within a second step these density values are used in order to determine a smooth iso-line to describe the boundary of the optimization layout. The nodal densities are now utilized to move this boundary on a fixed grid.

2. NODAL-BASED TOPOLOGY OPTIMIZATION PROBLEM

2.1 Optimization Problem Statements

In this paper, a linear elastostatic problem is considered for the structural topology optimization. In continuous formulations of the topology optimization problem, the design is given by a continuous scalar function $0 \le \Phi \le 1$ in the fixed design domain

$\Omega_x \subseteq \Re^n$ (n=2 or 3). The schematic of topology optimization of a solid structure with specified field and boundary conditions is shown in Figure 2.

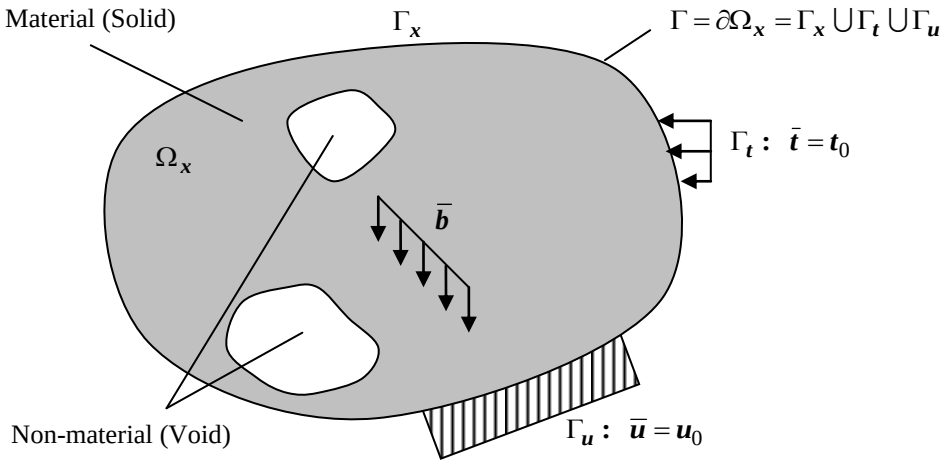

Fig 2. The schematic for topology optimization of structure

The general problem of structural topology optimization is specified as the objective function and constraints. According to a principle of minimum potential energy and regularization by a moved and regularized Heaviside function (MRHF) Ψ (Lee et al. 2007) as stated in Section 2.2.2, the objective function is written as a minimal strain energy form as follows.

$$f = \min\left[-\frac{1}{2} \int_{\Omega_x} \delta\varepsilon^T C\varepsilon \ \Psi(\Phi) \ d\Omega_x \right] \tag{1}$$

Here, according to discretization, the continuous material tensor C is dependent on the density-stiffness relationship of typical SIMP approach. Discontinuous Heaviside function is regularized as a smoothed and continuous form of MRHF. The function can be included in strain energy formulation, since it is based on signals of void (0) and solid (1) with respect to original Heaviside function.

The inequality optimization constraint is $0 \le \Phi \le 1$. Equality constraints are linear elastostatic equilibrium and the limit on the required amount of materials in terms of the constant volume V_0 of design domain as follows, respectively.

$$\int_{\Omega_x} \delta\varepsilon^T \sigma \ \Psi(\Phi) \ d\Omega_x = \int_{\Omega_x} \delta u^T \bar{b} \ d\Omega_x + \int_{\Gamma_t} \delta u^T \bar{t} \ d\Gamma_t \tag{2}$$

$$\int_{\Omega_x} d\Omega_x - V_0 = 0 \tag{3}$$

After discretization process of the continuous design domain Ω_x, the material density Φ is constantly assigned as Φ_i of each finite element i in order to calculate structural analyses of element level such as finite element method. For example, in case of square element with 4-node, it is averaged by 4 nodal densities of each finite element.

The averaged element density is defined by applying a penalty contour to the design variable field, *i.e.* as in the so-called "power law approach" or SIMP approach. According to the approach, the material density distribution has an effect on the element stiffness. Thus, the element stiffness-density relationship may be expressed in terms related to Young's modulus E, *i.e.* E_i is assigned by the updated element density Φ_i and is defined as

$$E_i(\Phi_i) = E_0\left(\frac{\Phi_i}{\Phi_0}\right)^k; \quad i = 1 \quad \cdots \quad n, \quad n = \textit{total number of element} \tag{4}$$

where E_0 and Φ_0 are respectively nominal values of Young's modulus and material density. The penalty parameter $k \geq 1$ penalizes intermediate material densities. Figure 3 shows penalty relationship between Young's modulus and element density according to various penalty parameters.

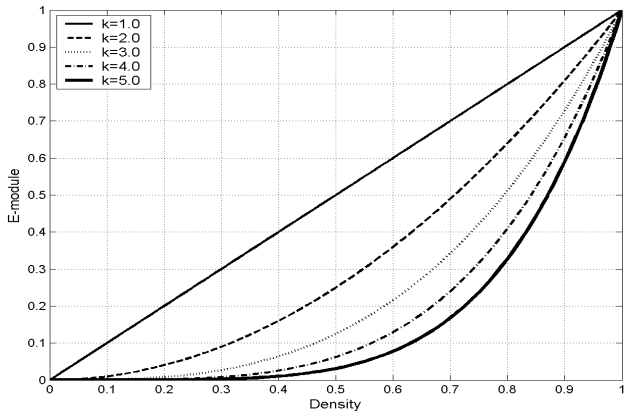

Fig 3. Penalty relationship between Young's modulus and element density

For example, and without loss of generality, an isotropic material model with a plane stress (such as a wall structure) is used here, so that

$$\boldsymbol{C}_i = \frac{\boldsymbol{E}_i(\Phi_i)}{1-\nu^2}\begin{bmatrix} 1 & \nu & 0 \\ \nu & 1 & 0 \\ 0 & 0 & \dfrac{1-\nu}{2} \end{bmatrix} \tag{5}$$

where $\boldsymbol{C}_i$ is a material tensor of each finite element $\boldsymbol{i}$ and includes the updated term of Young's modulus $\boldsymbol{E}_i$ defined by the updated element density Φ_i. ν is Poisson's ratio.

2.2 Geometric Interface Representation

2.2.1 Definition of Design Domain using 0.5 Iso-line

The design domain for material distribution problems of topology optimization can be divided into solid (1) and void (0) phases through signals of Heaviside function and is shown in Figure 4.

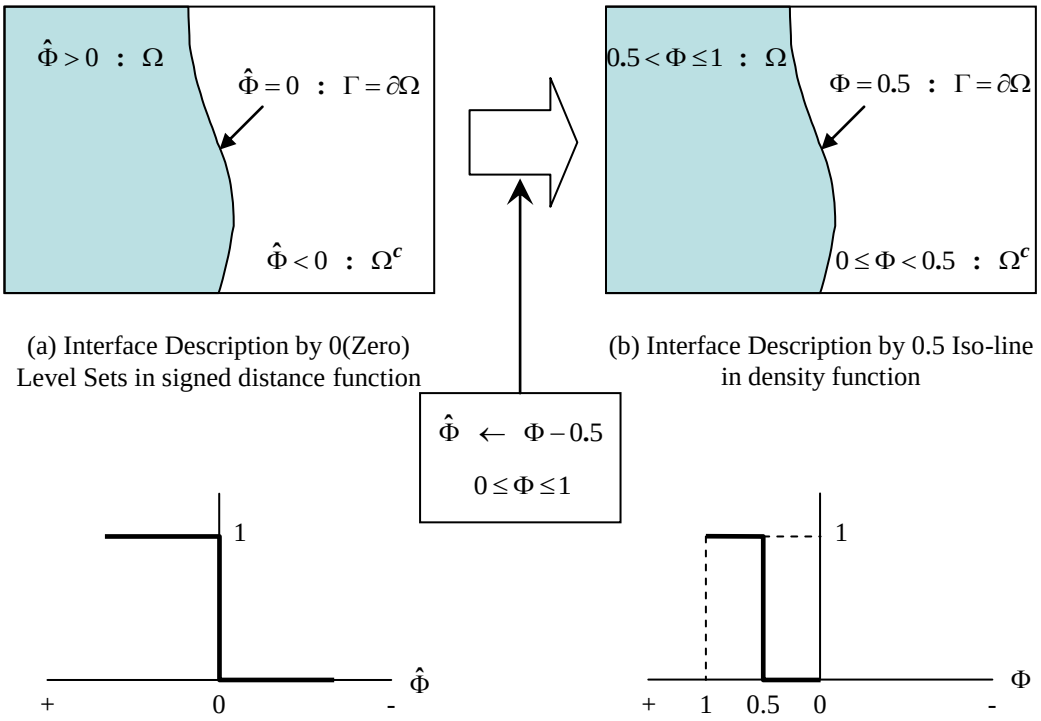

Fig 4. Geometric design domain and Heaviside function

Figure 4 (a) illustrates a boundary representation by zero level sets of a signed distance function which is well-known as level set methods (Allaire et al. 2004; Sethian and Wiegmann 2000; Shojaee and Mohammadian 2012; Dijk et al. 2012) and Figure 4 (b) shows the definition of interfaces between voids and solids by iso-line with a specific value 0.5 of density function. In this study, 0.5 iso-line in Figure 4 (b) is utilized for the smooth boundary representation. When densities of finite elements are smaller than 0.5, the regions are regarded as void phases in design domain. In the other hand, the regions whose densities are over 0.5 indicate solids. The design domain of 0.5 iso-line

Φ is obtained by mathematical transformation, *i.e.* $\hat{\Phi} \leftarrow \Phi - 0.5$ and $0 \le \Phi \le 1$ of the design domain of zero level sets $\hat{\Phi}$.

Figure 5 illustrates the process of constructing the 0.5 iso-line based on nodal densities as design parameters. It is assumed that element densities are assigned into nodal densities. A three-dimensional density function is bilinearly interpolated by the nodal densities. Then it is cut by a specific level of 0.5 and the boundaries between void and solid are described as 0.5 iso-lines. While the nodal densities is automatically updated during optimization processes, the boundaries by iso-lines can be propagated or reduced with changes of topology that it is possible to create voids in solid regions or solids in void regions.

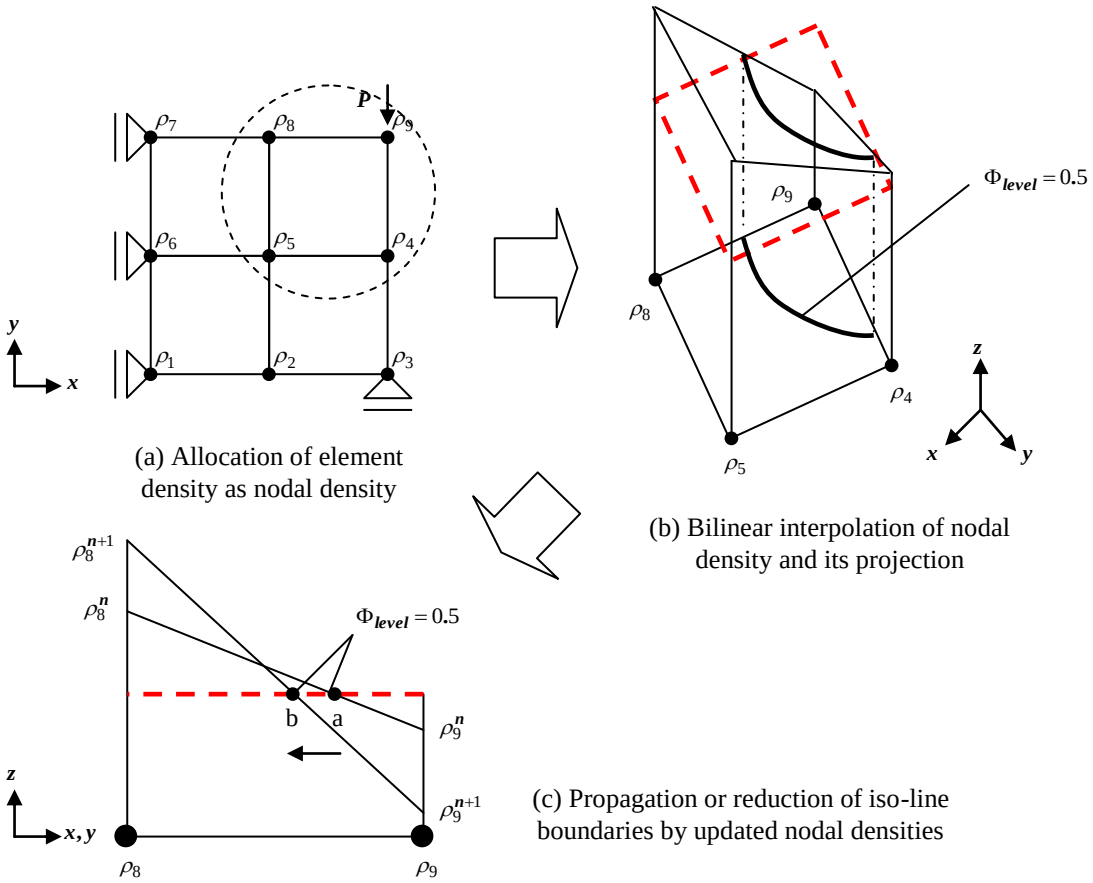

(a) Allocation of element density as nodal density

(b) Bilinear interpolation of nodal density and its projection

(c) Propagation or reduction of iso-line boundaries by updated nodal densities

Fig 5. The construction of iso-line by bilinear interpolation function

Figure 6 shows the interfaces propagated in discrete design domain during optimization iterations. Inactive elements have four nodal densities over or under the value of 0.5; otherwise, they are named as active elements. The inactive elements do not take part in the construction of the 0.5 iso-line interface, while the interfaces become yielded through updated density function of active elements during optimization iterations. Dash and bold lines show interfaces by $\boldsymbol{n}$ and $\boldsymbol{n+1}$ iteration, respectively.

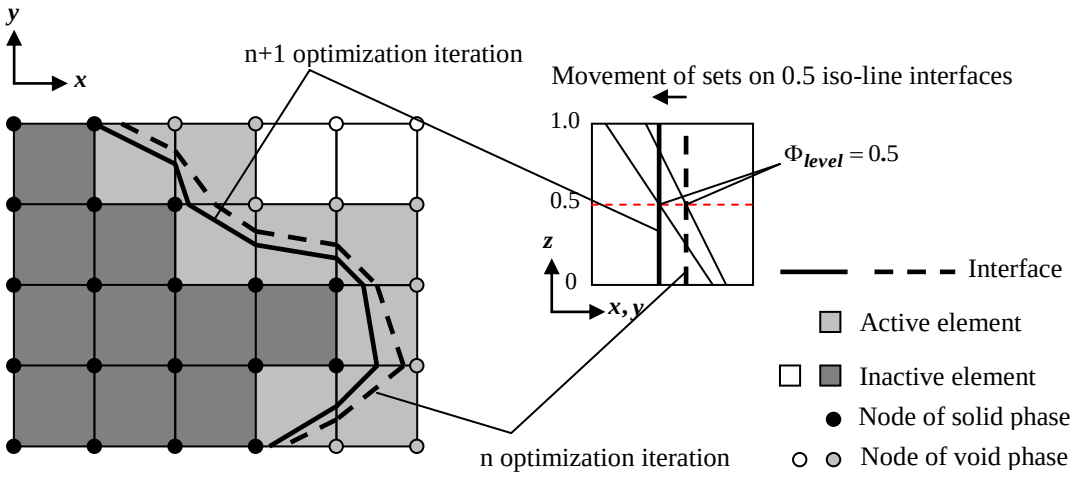

Fig 6. The propagation of interfaces in discrete design domain

2.2.2 Application of Moved and Regularized Heaviside Function

In material topology optimization problem, an indication function which decides material and no material phases in design domain can be described by Heaviside function [6]. In this study, since interfaces between materials and no materials are divided by 0.5 iso-lines in domain $0 \le \Phi \le 1$, Heaviside function (HF) is moved and constructs a moved Heaviside function (MHF) as shown in Figure 7.

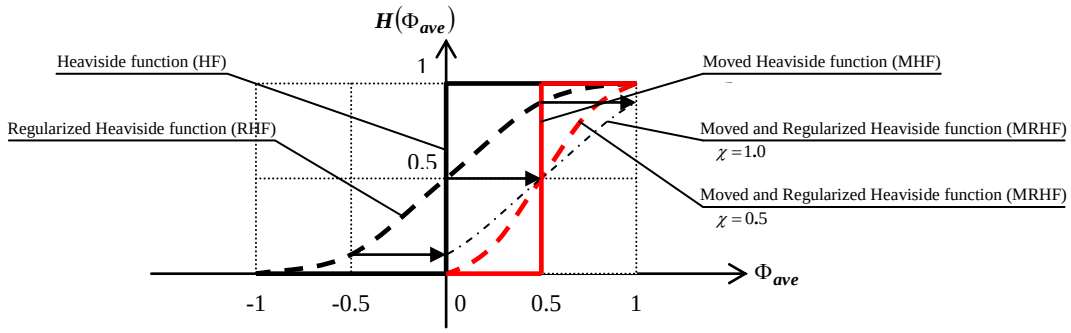

Fig 7. Moved and regularized Heaviside function (MRHF) (Lee et al. 2007)

The moved Heaviside function must be regularized in order to obtain numerical stability of calculation of sensitivities of objective function, where the regularization of Heaviside function has been introduced by Belytschko et al. in 2003. In this study, the function is named as a moved and regularized Heaviside function (MRHF) and it is illustrated in Figure 7. Here, χ is a regularization parameter with the value 0.5 or 1.0. The magnitude of MRHF depends on design variable values, *i.e.* here element density functions $\Phi_{ave}(\mathbf{x})$ averaged by four nodal densities, while a RHF is related to signed distance function in the work of Belytschko et al. In the present work, various types of MRHF of Equation (6) ~ (9) were devised and can be applied in order to regularize Heaviside function. The forms of MRHF are sketched in Figure 8.

$$\Psi_1(\Phi_{ave}) = \frac{3}{4}\left[\frac{\Phi_{ave}-0.5}{\chi} - \frac{1}{3}\left(\frac{\Phi_{ave}-0.5}{\chi}\right)^3\right] + \frac{1}{2} \tag{6}$$

$$\Psi_2(\Phi_{ave}) = \frac{1}{2} + \frac{2}{\pi}\mathbf{arctan}\left(\frac{\Phi_{ave}-0.5}{\chi}\right) \tag{7}$$

$$\Psi_3(\Phi_{ave}) = \frac{1}{2}\left[1 + \frac{\Phi_{ave}-0.5}{\chi} + \frac{1}{\pi}\mathbf{sin}\left(\frac{\pi(\Phi_{ave}-0.5)}{\chi}\right)\right] \tag{8}$$

$$\Psi_4(\Phi_{ave}) = \frac{1}{2}\left[1 + \mathbf{sin}\left(\frac{\pi(\Phi_{ave}-0.5)}{2\chi}\right)\right] \tag{9}$$

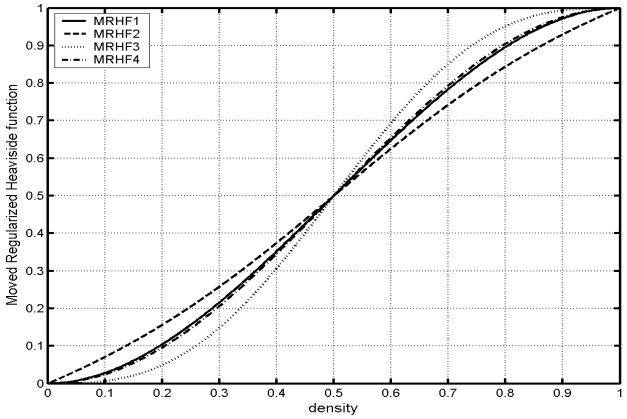

Fig 8. MRHF curves of Equation (6) ~ (9)

2.3 Discrete Formulation for Variational Sensitivity Analysis

In general, the sensitivity of optimization problems such as objective functions or constraints can be calculated by analytical or numerical method. Since sensitivity errors of the numerical sensitivity method may become great, the method is often used for verification of solutions. The analytical method is usually proper for the sensitivity of optimization problem due to small error of solutions. The analytical sensitivity method is distributed as a discrete and a variational approach. In the discrete approach, optimization problems are at first discretized and then derivative is carried out. However, the variational approach firstly differentiates continuous optimization problems and secondly the derivative is discretized.

The analytical sensitivity method of the variational approach is utilized here, since the variational method is numerically more efficient than discrete method in certain optimization problems and large number of design parameters, which is stated by Schwarz in 2001. Since continuous displacement fields depend on design variables s (for instance, material densities), the total differential form of the objective function consists of parts of an explicit partial derivative and an implicit partial derivative, and it is defined as introduced by Haug et al. in 1986.

$$\nabla_s \boldsymbol{f} \;=\; \nabla_s^{ex} \boldsymbol{f} \;+\; \overline{\nabla}_u \boldsymbol{f}^T \nabla_s \boldsymbol{u} \tag{10}$$

The total partial derivative is written as

$$\nabla_s \boldsymbol{f} = \frac{1}{2}\int_{\Omega_x} \varepsilon^T \nabla_s \boldsymbol{C}(\Phi)\varepsilon \;\Psi(\Phi)\; d\Omega_x + \frac{1}{2}\int_{\Omega_x} \varepsilon^T \boldsymbol{C}(\Phi)\varepsilon \;\nabla_s \Psi \; d\Omega_x + \frac{1}{2}\int_{\Omega_x} \varepsilon^T \boldsymbol{C}(\Phi)\nabla_u \varepsilon \;\Psi(\Phi)\nabla_s \boldsymbol{u} \; d\Omega_x \tag{11}$$

where $\nabla_s \Psi(\Phi)$ denotes a derivative of MRHF, *i.e.* a moved and regularized Dirac delta function (MRDDF). Through derivative of equilibrium of Equation (2) satisfying field and boundary conditions, the term of a derivative of continuous displacement fields $\nabla_s \boldsymbol{u}$ by design variables can be written as

$$\begin{aligned}
&\int_{\Omega_x} \delta \boldsymbol{u}^T \boldsymbol{L}^T \boldsymbol{C}(\Phi)\boldsymbol{L}\;\Psi(\Phi)\nabla_s \boldsymbol{u}\; d\Omega_x = \int_{\Omega_x} \delta \boldsymbol{u}^T \nabla_s \bar{\boldsymbol{b}}\; d\Omega_x + \int_{\Gamma_t} \delta \boldsymbol{u}^T \nabla_s \bar{\boldsymbol{t}}\; d\Gamma_t \\
&- \int_{\Omega_x} \delta \boldsymbol{u}^T \nabla_s \boldsymbol{L}^T \boldsymbol{C}(\Phi)\boldsymbol{L}\boldsymbol{u}\;\Psi(\Phi)\; d\Omega_x - \int_{\Omega_x} \delta \boldsymbol{u}^T \boldsymbol{L}^T \nabla_s \boldsymbol{C}(\Phi)\boldsymbol{L}\boldsymbol{u}\;\Psi(\Phi)\; d\Omega_x \\
&- \int_{\Omega_x} \delta \boldsymbol{u}^T \boldsymbol{L}^T \boldsymbol{C}(\Phi)\nabla_s \boldsymbol{L}\boldsymbol{u}\;\Psi(\Phi)\; d\Omega_x - \int_{\Omega_x} \delta \boldsymbol{u}^T \boldsymbol{L}^T \boldsymbol{C}(\Phi)\boldsymbol{L}\boldsymbol{u}\;\nabla_s \Psi(\Phi)\; d\Omega_x
\end{aligned} \tag{12}$$

In order to calculate the derivative of continuous displacement fields $\nabla_s \boldsymbol{u}$, an adjoint method is used here. The adjoint method does not have to directly calculate continuous displacement fields with great numerical consuming. A new objective function is defined as

$$\bar{\boldsymbol{f}} = \boldsymbol{f} - \lambda\left[\int_{\Omega_x} \delta\varepsilon^T \sigma\;\Psi(\Phi)\; d\Omega_x - \int_{\Omega_x} \delta \boldsymbol{u}^T \bar{\boldsymbol{b}}\; d\Omega_x - \int_{\Gamma_t} \delta \boldsymbol{u}^T \bar{\boldsymbol{t}}\; d\Gamma_t\right] \tag{13}$$

where the renewed objective function $\bar{\boldsymbol{f}}$ has an additional 0-term of static equilibrium, which is multiplied with a Lagrangian multiplier λ. The derivative of the Lagrangian multiplier λ disappears because of the 0-term. Therefore the derivative of Equation (13) is written as

$$\nabla_s \overline{\overline{f}} = \nabla_s^{ex} f + \overline{\nabla}_u f^T \nabla_s u - \lambda \int_{\Omega_X} \delta u^T L^T C(\Phi) L \, \Psi(\Phi) \, \nabla_s u \, d\Omega_x$$

$$\underline{\qquad\qquad\qquad\qquad\qquad\qquad\qquad\qquad\qquad\qquad\qquad\qquad\qquad\qquad\qquad\qquad} (a)=0$$

$$- \lambda \int_{\Omega_X} \delta u^T \nabla_s L^T C(\Phi) L u \, \Psi(\Phi) \, d\Omega_x - \lambda \int_{\Omega_X} \delta u^T L^T \nabla_s C(\Phi) L u \, \Psi(\Phi) \, d\Omega_x$$

$$- \lambda \int_{\Omega_X} \delta u^T L^T C(\Phi) \nabla_s L u \, \Psi(\Phi) \, d\Omega_x - \lambda \int_{\Omega_X} \delta u^T L^T C(\Phi) L u \, \nabla_s \Psi(\Phi) \, d\Omega_x$$

$$+ \lambda \int_{\Omega_X} \delta u^T \nabla_s \bar{b} \, d\Omega_x + \lambda \int_{\Gamma_t} \delta u^T \nabla_s \bar{t} \, d\Gamma_t \tag{14}$$

Lagrangian multipliers λ take arbitrary values. A specific Lagrangian multiplier value can be determined in Equation (14) in order to remove the derivative of continuous displacement fields which is numerically very expensive. Therefore a specific equation (a) = 0 in Equation (14) is made to include the specific Lagrangian multiplier value. After discretization of continuous design domain, the specific equation with a satisfied Lagrangian multiplier is expressed as

$$\hat{u}^T \int_{\Omega_\xi} B^T C(\Phi_i) B |J| \Psi(\Phi_i) \, d\Omega_\xi \nabla_s \hat{u} - \lambda \, \delta\hat{u}^T \int_{\Omega_\xi} B^T C(\Phi_i) B |J| \Psi(\Phi_i) \, d\Omega_\xi \nabla_s \hat{u} = 0 \tag{15}$$

Through Equation (15), the required Lagrangian multiplier value is obtained and the value is substituted for discrete form of Equation (14). Under the assumptions that body force $\bar{b}$, traction force $\bar{t}$, differential matrix L and Jacobi matrix J are independent of design variables s, the total partial derivative of the objective function can be simply rewritten as follows.

$$\nabla_s \overline{\overline{f}} = -\frac{1}{2} \hat{u}^T \int_{\Omega_\xi} B^T \nabla_s C(\Phi_i) B |J| \, \Psi(\Phi_i) \, d\Omega_\xi \hat{u}$$

$$-\frac{1}{2} \hat{u}^T \int_{\Omega_\xi} B^T C(\Phi_i) B |J| \, \nabla_s \Psi(\Phi_i) \, d\Omega_\xi \hat{u} \tag{16}$$

It seems that Equation (16) is related to the characteristics of both topological and shape derivatives. Note that the topological derivative (Sokolovski and Zochowski 1999; Novotny et al. 2003; Guo et al. 2005) are proportional to updated design variable Φ_i and therefore the first term of Equation (16) is similar to the topological derivative. According to this derivative, voids can be created in solid regions and solids can grow up from void regions. This point is based on typical topology optimization. The value of

MRDDF exists in only $\Phi_i = 0.5$, which yields iso-line interfaces between material and no material regions. MRDDF disappears at $\Phi_i \neq 0.5$. Thus the second term of Equation (16) can be named as a kind of shape derivatives (Guo et al. 2005). It is based on boundary variation of shape optimization.

The topological and shape derivatives of Equation (16) imply that the present approach is a form of combined topology and shape optimization. It removes the defect of shape derivative that it is usually very difficult or impossible to create holes within existing shapes away from the interfaces and results in fast convergence in terms of numerical aspect and optimal structure with maximal stiffness with respect to physical points.

3. NUMERICAL EXAMPLES

3.1 Topology Optimization of MBB-beam

3.1.1 Problem definition

As a test example, a MBB-beam as shown in Figure 9 is considered to valuate the present method. For numerical efficiency, a half part of MBB-beam is calculated.

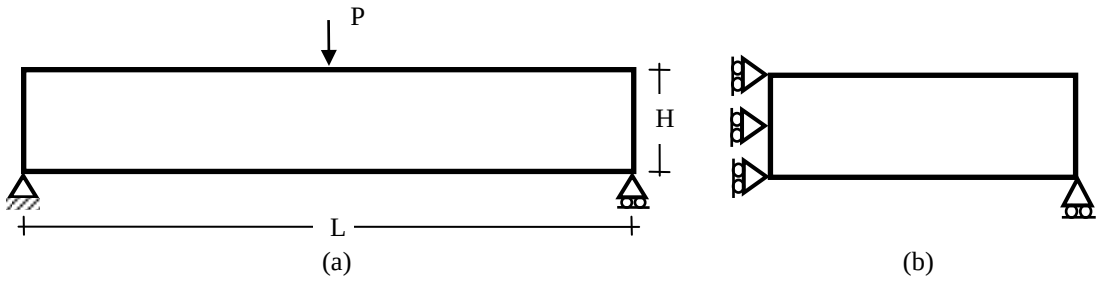

Fig 9. Analysis model (a) MBB-beam (b) half MBB-beam

30×10, 60×20 and 90×30 finite elements of square with 4 nodes are utilized for discretization of design domain (L/2(6m) × H/2(2m)). For numerical simplicity, material parameters are Young's modulus $\boldsymbol{E} = 1.0\ \boldsymbol{kN/m^2}$ and Poisson's ratio $\nu = 0.2$. An applied load of $\boldsymbol{P} = 1.0\ \boldsymbol{kN}$ is concentrated at the center of upper surface in structure.

The penalty parameter of $\boldsymbol{k} = 5.0$ is used for SIMP approach. The penalty formulation includes pure element densities in element-based topology optimization and averaged element densities in nodal-based topology optimization. The objective function is minimal strain energy and the volume of 50% is fixed during the whole optimization procedures. For the present approach, MRHF of Equation (6) with $\chi = 0.5$ is used into the defined optimization problem.

Table 1 shows the problem types of typical element-based topology optimization (EBTO), typical nodal-based topology optimization (NBTO) and nodal-based topology

optimization (NBTO) using MRHF. Here, Matlab codes (Sigmund 2001) are utilized in order to execute topology optimization.

Table 1. Problem types of topology optimization

Topology Optimization	Type of SIMP	Design variable	Indication
Element-based design	Typical	Element density	EBTO
Nodal-based design	Typical	Nodal density (Average element density)	NBTO
Nodal-based design	Regularization (MRHF)	Nodal density (Average element density)	NBTO-MRHF

3.1.2 Comparisons between original EBTO and original NBTO

When different discretization of design domain is considered, convergent histories of objective function in element and nodal-based topology optimization are shown in Figure 10. It can be found that the changing values of objective in NBTO have slower streams than those in EBTO since not element densities but averaged element densities are design variables in NBTO and changes of the variable values are slow. In addition, NBTO requires many design parameters, *i.e.* nodal densities in order to carry out sensitivity analyses and optimization methods such as OC or MMA. Therefore convergence of NBTO is not good and basically it is a disadvantage of NBTO.

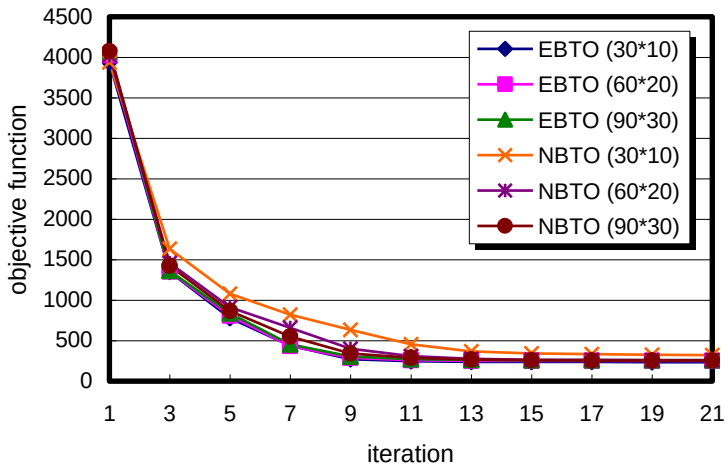

Fig 10. The histories of convergence in EBTO and NBTO

Generally, design domain is the more discretized, solutions of structural behaviors become the more close to exact values. Therefore convergent values in EBTO and NBTO are converged as specific values in increasing discretization. The specific values are close to exact convergent values.

Figure 11 shows convergent objective function values under different discretization in EBTO and NBTO. Contrary to NBTO, in EBTO it can be seen that convergent values of maximal stiffness decrease gradually, while the finite elements become refined.

Finally EBTO yields optimal structures with lower stiffness as convergent values than NBTO. The results of EBTO may not take structural reliability about safety.

Its reason is related to numerical instability such as a local minimum or oscillation of convergent values. However NBTO reduces the numerical instability by redistributing averaged element densities through nodal densities. The fact presents an important reason which NBTO can be utilized instead of EBTO, although NBTO has slow convergence and computational burdens.

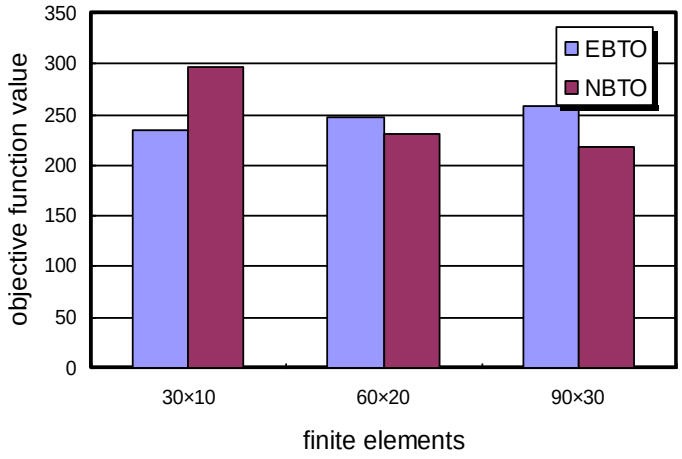

Fig 11. The convergent values of objective function in EBTO and NBTO

3.1.3 Results of NBTO using MRHF

Figure 12 illustrates histories of convergence in typical NBTO without MRHF and NBTO using MRHF. It can be seen that the convergences of NBTO using MRHF are superior to those of original NBTO without MRHF. It seems to be even better than convergences of EBTO in case of 60×20 and 90×30 finite elements.

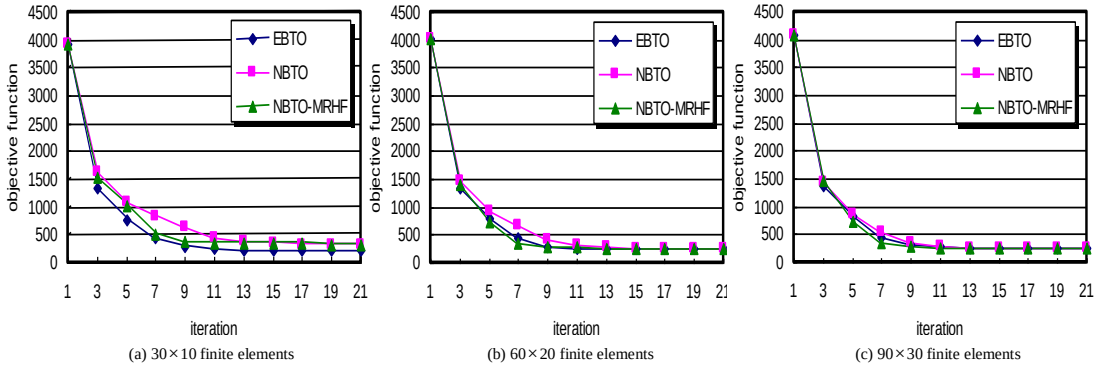

Fig 12. The histories of convergence in original NBTO without MRHF and NBTO using MRHF

Optimal contours of density distribution and continuous 0.5 iso-lines in MBTO without MRHF and NBTO using MRHF under 90×30 finite elements are shown in Figure 13. It can be seen that different topologies, *i.e.* connectivity of material

distributions, are yielded and according to analytical solutions of MBB-beam optimal topologies of NBTO without MRHF seems to be better than those of NBTO using MRHF.

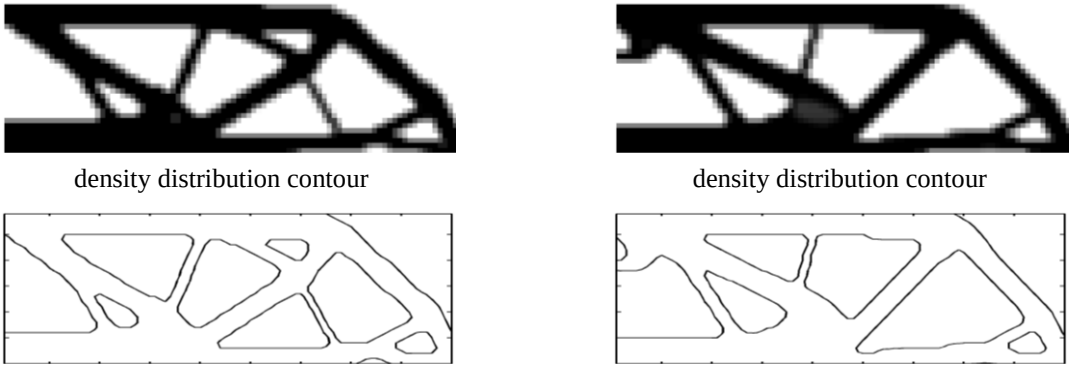

(a) NBTO without MRHF (b) NBTO using MRHF

Fig 13. Optimal density distribution contours in 90×30 finite elements

The good convergence of NBTO using MRHF compared to original EBTO and original NBTO without MRHF is related to characteristics of sensitivity analyses. The sensitivity of the present approach implies the combination of topological and shape derivatives as stated in Equation (16) for sensitivity.

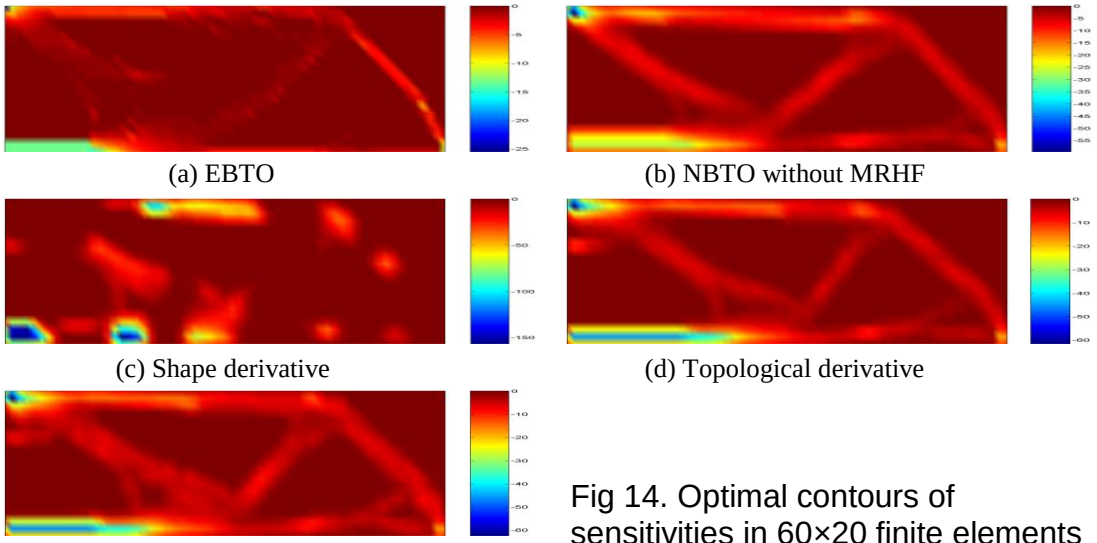

(a) EBTO (b) NBTO without MRHF

(c) Shape derivative (d) Topological derivative

(e) NBTO using MRHF = (c) + (d)

Fig 14. Optimal contours of sensitivities in 60×20 finite elements

The first term of Equation (16) is the topological derivative since it is proportional to design variables such as typical EBTO. The second one is regarded as the shape derivative because Dirac delta function, *i.e.* a derivative of Heaviside function, has existence on only 0.5 iso-line interface of density function. Optimal contours of the

sensitivities in EBTO, NBTO without MRHF and NBTO using MRHF are shown in Figure 14.

Figure 15 illustrate 0.5 iso-line interfaces changed by iterations in NBTO and NBTO using MRHF. It can be found that topology of structure is more fast yielded in NBTO using MRHF than in NBTO without MRHF.

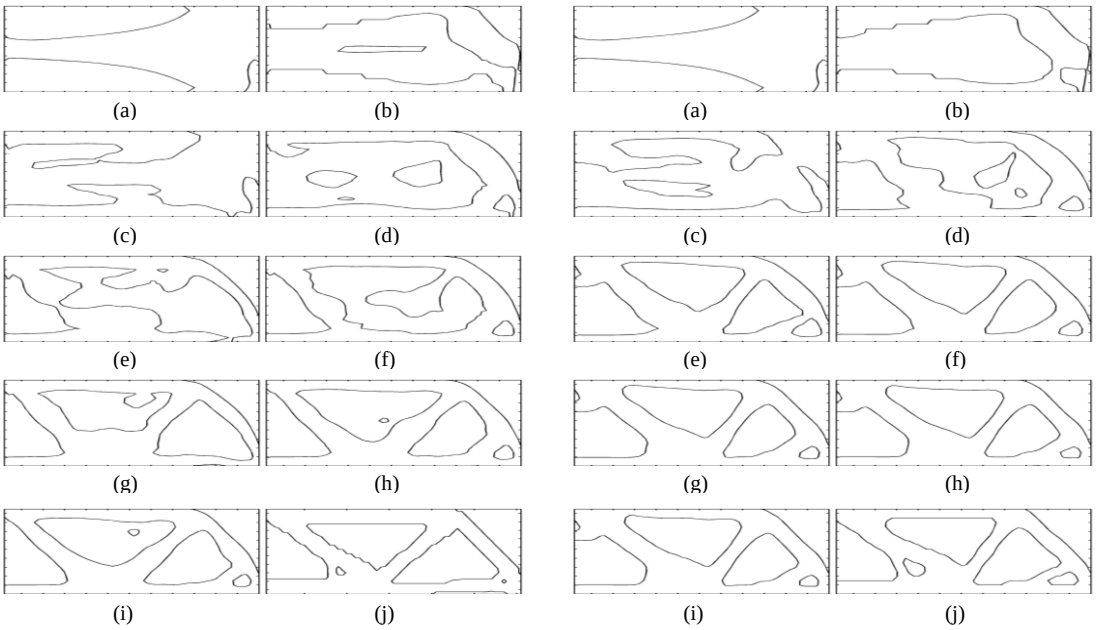

Fig 15. 0.5 iso-line interfaces of each iteration in 60×20 finite elements
(a) initial stage (b) ~ (i) intermediate stages (j) final stage

4. CONCLUSIONS

In this study, a combined topology and shape optimization is proposed in linear elastostatic structures, which yields both the generation of smooth shape and the determination of optimal topology.

At first in order to obtain optimal topology, it is based on a design domain concept of a density distribution method such as SIMP. Nodal densities of material properties are considered as design parameters. Element densities which are averaged by the nodal densities are utilized for finite element analysis. Optimal density contours are distributed into fixed grids by the constant and averaged element densities. At second for the purpose of yielding optimal smooth shape, the nodal densities are bilinearly interpolated by element shape functions and then a 3 dimensional density function is constructed in design domain. 0.5 level of the density function values is not only smooth iso-line contours but also material interfaces between void and solid regions. These optimal shape and topology are stimulated in fixed grids. This method allows us perform a combined topology and shape optimization on this grid with smooth boundaries which can be easily implemented in existing gradient-based optimization codes.

In compared with typical EBTO, a convergence of original NBTO may be slow since the present approach requires many design parameters and changes of the averaged variable values are very slow. In order to reduce the problems, a moved and regularized Heaviside function is implemented to the proposed approach. As a consequence, a topological as well as a shape derivative is executed for sensitivity analyses. Then it is possible to create voids in solids or solids in voids under boundary-based variations of smooth interfaces.

A numerical example of MBB-beam verified the efficiency of the combined topology and shape optimization with nodal density as design parameter.

ACKNOWLEDGMENTS

This research was supported by the MKE (The Ministry of Knowledge Economy), Korea, under the Convergence-ITRC (Convergence Information Technology Research Center), supervised by the NIPA(National IT Industry Promotion Agency), (NIPA-2013-H0401-13-1003) and a grant (code# 2010-0019373, 2011-0010300, 2012R1A2A1A01007405 & 2013-057502) from the National Research Foundation of Korea (NRF) funded by the Korea government.

REFERENCES

Maute, K., Schwarz, S. and Ramm, E. (1998), “Adaptive Topology Optimization of Elastostatic Structures”, *Structural Optimization*, **15**, 81-91.

Kemmler, R., Lipka, A. and Ramm, E. (2005), “Large Deformations and Stability in Topology Optimization”, *Structural and Multidisciplinary Optimization*, published online in Structural Optimization.

Schwarz, S., Maute, K. and Ramm, E. (2001), “Topology and Shape Optimization for Elastostatic Structural Response”, *Computer Methods in Applied Mechanics and Engineering*, **190**, 2135-2155.

Allaire, G., Jouve, F. and Toader, A.M. (2004), “Structural Optimization using Sensitivity Analysis and A Level-set Method”, *Journal of Computational Physics*, **194**(1), 363-393.

Sethian, J.A. and Wiegmann, A. (2000), “Structural Boundary Design via Level Set and Immersed Interface Methods”, *Journal of Computational Physics*, **163**(2), 489-528.

Belytschko, T., Xiao, S.P. and Parimi C. (2003), “Topology Optimization with Implicit Functions and Regularization”, *International Journal for Numerical Methods in Engineering*, **57**, 1177-1196.

Schwarz, S. (2001), *“Sensitivitätsanalyse und Optimierung bei Nichtlinearem Strukturverhalten”*, Ph.D Thesis, University of Stuttgart, Germany.

Haug, E.J., Choi, K.K. and Komkov, V. (1986), *“Design Sensitivity Analysis of Structural Systems”*, Academic Press, Orlando, New York.

Sokolovski, J. and Zochowski, A. (1999), “On the Topological Derivative in Shape Optimization”, *SIAM Journal on Control and Optimization*, **37**, 1251-1272.

Novotny, A.A., Feijoo, R.A., Taroco, E. and Padra, C. (2003), "Topological-Shape Sensitivity Analysis", *Computer Methods in Applied Mechanics and Engineering*, **192**, 803-829.

Guo, X., Zhao, K. and Wang, M.Y. (2005), "Simultaneous Shape and Topology Optimization with Implicit Topology Description Functions", *Control and Cybernetics, a Special Issue on Shape Optimization*, **34**(1), 255-282.

Sigmund, O. (2001), *"*A 99 Topology Optimization Code written in Matlab", *Structural and Multidisciplinary Optimization*, **21**, 120-127.

Lee, D.K., Shin, S.M. and Park, S.S. (2007), "Computational Morphogenesis Based Structural Design by Using Material Topology Optimization", *Mechanics Based Design of Structures and Machines*, **35**(1), 39-58.

Shojaee, S. and Mohammadian, M. (2012), "Structural topology optimization using an enhanced level set function", *Scientia Iranica*, **19**(5), 1157-1167.

Dijk, N.P.V., Langelaar, M. and Keulen, F.V. (2012), "Explicit level set-nased topology optimization using an exact Heaviside function and consistent sensitivity analysis", *International Journal for Numerical Methods in Engineering*, **91**(1), 67-97.